Drug Design, Development and Therapy

Dovepress
Taylor & Francis Group

Open Access Full Text Article

ORIGINAL RESEARCH

Mechanism of *SiMiaoWan* in the Treatment of Hyperuricemia Based on Serum Metabolomics

Mengping Guo[1], Bo Sun[2], Xiaochen Ding[2], Jingxiang Su[2], Xiuzhen Wang[1], Xiangjun Qiu[2]

[1]Department of Pharmacy, Luoyang Orthopedic-Traumatological Hospital of Henan Province, Henan Provincial Orthopedic Hospital Zhengzhou Campus, Zhengzhou, Henan, 450016, People's Republic of China; [2]College of Basic Medicine and Forensic Medicine, Henan University of Science and Technology, Luoyang, Henan, 471023, People's Republic of China

Correspondence: Xiuzhen Wang, Department of Pharmacy, Luoyang Orthopedic-Traumatological Hospital of Henan Province, Henan Provincial Orthopedic Hospital Zhengzhou Campus, Zhengzhou, Henan, 450016, People's Republic of China, Email wangxiuzhen86@163.com; Xiangjun Qiu, College of Basic Medicine and Forensic Medicine, Henan University of Science and Technology, Luoyang, Henan, 471023, People's Republic of China, Email lyxiangjun@126.com

Background: *SiMiaoWan* (SMW) can clear heat, expel dampness, tonify the kidney, strengthen the muscles, and treat damp heat in the spleen, stomach, and Lower Jiao. SMW is a formula commonly used for the clinical treatment of gout and hyperuricemia (HUA), especially asymptomatic HUA, and has shown remarkable therapeutic effects. This study aimed to investigate the therapeutic effect and mechanisms of SMW in a rat model of HUA using serum metabolomics.

Methods: Rats were administered high levels of uric acid (UA) to establish a model of hyperuricemia and subsequently treated with SMW. Then, the levels of the biochemical indicators serum uric acid (SUA), alanine aminotransferase (ALT), aspartate transaminase (AST), urea nitrogen (BUN), and creatinine (CRE) were measured, and histological analysis of stained liver and kidney tissue sections was performed. Furthermore, blood samples were collected after the animal experiment for serum untargeted metabolomics analysis via ultra-performance liquid chromatography–tandem mass spectrometry (UPLC–MS/MS) and subsequent Kyoto Encyclopedia of Genes and Genomes (KEGG) enrichment pathway analysis.

Results: The levels of the biochemical indicators were significantly lower in rats treated with SMW than in control rats. Additionally, metabolomics and KEGG enrichment pathway analyses indicated that central carbon metabolism, protein digestion and absorption, and amino acid biosynthesis pathways may play important regulatory roles in the SMW-mediated lowering of the SUA level in hyperuricemic rats.

Conclusion: SMW effectively reduced the SUA level in hyperuricemic rat models and alleviated the renal impairment induced by hyperuricemia. The mechanism of SMW is closely associated with pathways related to central carbon metabolism in cancer, protein digestion and absorption, and amino acid biosynthesis.

Keywords: *SiMiaoWan*, hyperuricemia, liver and kidney function, metabolomics, Kyoto Encyclopedia of Genes and Genomes

Introduction

Hyperuricemia (HUA), a common and potentially devastating chronic metabolic disease that has not attract much attention, is caused by dysregulated purine metabolism or the excessive production or/and excretion of uric acid (UA). The excessive intake of purine-rich foods and disturbances in purine metabolism are the two main causes of excessive UA production. Additionally, prevalence of HUA in China has increased annually, and HUA has gradually began affecting younger individuals. Thus, HUA has become the second most common metabolic disease after diabetes mellitus and a major public health concern.[1] Moreover, HUA is closely related to the development of other diseases. In this study, HUA treatment was studied.

SiMiaoWan (SMW) consists of four Chinese herbs, namely, *Huang Bai* (*Phellodendron amurense), Cang Zhu* (Rhizoma atractylodis), *Niu Xi* (Radix achyranthis bidentatae) and *Yi Yi Ren* (coix seed).[2] SMW is a yellowish-brown water pill with the slight effect of gas and a bitter and astringent taste. *Huang Bai* is the medicinal herb component of SMW, and its cold is used to overcome heat, while its bitterness is used to dry dampness; moreover, Huang Bia can

Received: 28 April 2025
Accepted: 28 June 2025
Published: 7 July 2025

Graphical Abstract

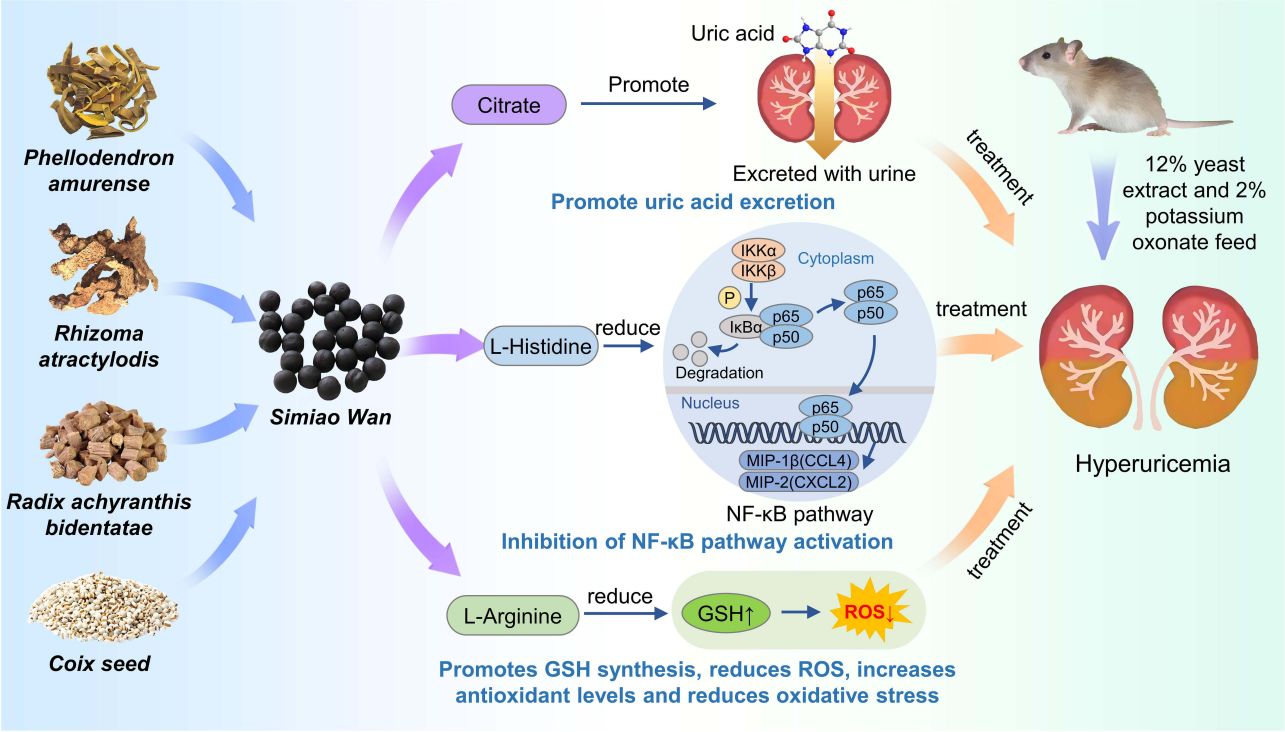

remove damp heat from the Lower Jiao. Additionally, *Cang Zhu* is a bitter and warm common medicinal herb that can invigorate the spleen, dry dampness, and relieve rheumatism. Furthermore, *Niu Xi* promotes blood circulation and meridians, nourishes the liver and kidneys, strengthens muscles and bones. Finally, *Yi Yi Ren*, the only component that enters Yang Ming, dispels dampness and heat while improving the tendons and collaterals. When combined with other medicines, *Yi Yi Ren* assists in clearing heat and dampness, nourishing the kidneys and strengthening the tendons.[3] In traditional Chinese medicine clinical practice, SMW has been confirmed to effectively treat HUA and various types of arthritis, although its pharmacological mechanism has not been fully elucidated.[4] Therefore, in this experimental study, the pharmacological mechanism of SMW in treating HUA will be further investigated and analyzed.

Metabolomics is applied to investigate the various endogenous small molecule (molecular weight less than 1000 Da) metabolites present in the body (tissues, organs, body fluids, cells, etc.) through data analysis and rapid detection techniques and to determine the differences and changes in metabolite contents after different treatments or in various states of the body. Metabolomics is a continuously and rapidly developing omics method that can be used to evaluate the dynamic changes in endogenous metabolites and explore potential physiological and pathological mechanisms in depth.[5] In this study, the differences in metabolites among different treatment groups was compared via nontargeted metabolomics, and the metabolites and metabolic pathways related to HUA were identified, analyzed, and discussed.

Materials and Methods

Chemicals and Reagents

Acetonitrile (lot: 1.00030.4008), methanol (lot: 1.06007.4008), and formic acid (lot: 111670) were purchased from Millipore (Massachusetts, MA, USA). Ammonia (lot: 105426) was obtained from Merck (Darmstadt, Germany). Benzbromarone tablets (lot: 20220412) were purchased from Changzhou Kangpu Pharmaceutical Co., Ltd. (Jiangsu, China), and SMW (lot: 220725) was procured from Jilin Zixin Pharmaceutical Co., Ltd. (Jilin, China).

Experimental Animal Selection and Grouping

In this experiment, 60 adult male Sprague–Dawley (SD) rats with body weights of 200 ± 20 g were used (Huaxing Experimental Animal Farm, Huiji District, Zhengzhou City; license number SCXK (Henan) 2019–0002). This study was approved by the Animal Laboratory of Henan University of Science and Technology (202210002) and followed the Guidelines for Ethical Review of Laboratory Animals Welfare (GB/T35892-2018). The animals were kept in the environmental control room for at least 7 d before the experiment began under the following conditions: temperature, 22 ± 2 °C; humidity, 50 ± 10%; and light/dark cycle, 12 h. Before the experiment, the animals were fasted for 12 h but allowed free access to drinking water.

The 60 adult male SD were randomly divided into a blank group (Group A), a hyperuricemic model group (Group B), a benzbromarone positive control group (Group C), a high-dose SMW group (Group D), a medium-dose SMW group (Group F), and a low-dose SMW group (Group G) with a total of 10 animals in each group. The blank group was given normal feed and free access to drinking water, whereas the other groups were given feed containing 12% yeast extract and 2% potassium oxonate for 5 consecutive weeks to establish a model of HUA. After the 5th week, blood was collected from each group of rats via the tail vein to measure SUA levels; an increase of more than 20% compared with that of the blank group indicated that modeling was successful. Next, all groups were fed the standard feed given to the blank group, and gavage treatment was initiated. The rats in the benzbromarone positive control group were given 5 mg/kg benzbromarone once a day for 4 consecutive weeks, the rats in the high-, medium-, and low-dose SMW groups were given 2.52 g/kg, 1.26 g/kg, and 0.63 g/kg SMW, respectively, for 4 consecutive weeks, and the rats in the blank and the hyperuricemic model groups were administered the same volume of physiological saline. After treatment was completed, blood samples were collected from the rats in all the groups via the tail vein for subsequent biochemical analyses. Additionally, liver and kidney tissues were randomly collected from each group of rats, and their wet weights and corresponding indices were measured. Finally, venous blood samples were collected again from the blank, HUA model, and SMW medium-dose groups for subsequent metabolomics analysis.

Excluding accidents during the experimental process, each group of experimental animals was guaranteed to have 8 animals, that is, each group has 8 different samples for biochemical testing and metabolomics analysis.

Determination of the Rat Organ Coefficients

After blood collection, the rats were anesthetized via intraperitoneal injection of 3% pentobarbital sodium at a dose of 30 mg/kg. The rats were subsequently dissected, and the livers and kidneys were separated. The separated organs were washed with physiological saline, dried with filter paper, and weighed. Finally, the liver and kidney coefficients were calculated.

Biochemical Indices

The serum samples were warmed to room temperature to ensure even thawing. Then, the SUA and serum levels of urea nitrogen (BUN), creatinine (CRE), aspartate aminotransferase (AST), and alanine aminotransferase (ALT) were measured according to the instructions of the automatic biochemical analyzer.

Data Processing and Analysis

The experimental data are presented as the mean plus or minus the standard deviation (X±SD) for each group of animals. The data were statistically analyzed using GraphPad Prism 9.5 software. One-way analysis of variance (ANOVA) and a multiple comparative analysis test were used to compare the data among multiple groups, and $P<0.05$ was considered to indicate statistical significance.

Metabolomics

In this study, serum samples from three groups, A (blank), B (HUA model), and F (medium-dose SMW), were selected for metabolomics analysis. Additionally, quality control (QC) samples were also collected and used to calibrate the chromatography–MS system and measurement equipment and to assess the stability of the system throughout the experiments.

The samples to be tested were thawed at 4 °C and mixed with a rotary mixer. Then, 400 μL of precooled pure methanol was added to 100 μL of each sample, followed by vortexing, thorough mixing and ultrasonication in an ice bath for 20 min. After storage at −20 °C for 1 h, the supernatant was separated by centrifugation at 16,000 × g for 20 min at 4 °C, and the solvent was evaporated using a high-speed vacuum centrifuge. Finally, 100 μL of a methanol:water mixture (1:1 v/v) was added to dissolve the residue, the mixture was centrifuged at 20,000 × g and 4 °C for 15 min, and the supernatant was analyzed via MS.

A SHIMADZU-LC30 ultrahigh-performance liquid chromatography (UHPLC) system and an ACQUITY UPLC® HSS T3 column (2.1 × 150 mm, 1.8 μm; Waters, Milford, MA, USA) were used for chromatographic separation. The automatic sampler temperature was set to 4 °C, and 4 μL of each sample was injected for analysis. The mobile phases were A (0.1% aqueous formic acid) and B (acetonitrile) with a flow rate of 0.3 mL/min. Additionally, the column temperature was set to 40 °C. Gradient elution was performed as follows: 0–2 min, 0% B; 2–6 min, linear increase from 0% to 48% B; 6–10 min, linear increase from 48% to 100% B; 10–12 min, maintained at 100% B; 12–12.1 min, linear decrease from 100% to 0% B; and 12.1–15 min, maintained at 0% B.

Electrospray ionization (ESI) was used for sample detection in both positive and negative ion modes. After UHPLC separation, further analysis was performed using a QE Plus mass spectrometer followed by ionization with an HESI source under the following conditions: spray voltage, 3.8 kV for positive mode and 3.2 kV for negative mode; capillary temperature, 320 °C; sheath gas, 30 arbitrary units; auxiliary gas, 5 arbitrary units; probe heater temperature, 350 °C; and S-Lens RF level, 50. MS data were acquired with the following parameters: acquisition time, 15 min; parent ion scanning range, 70–1050 m/z; primary MS resolution, 70,000 at m/z 200; AGC target, 3e6; and maximum IT, 100 ms. Secondary MS analysis was performed as follows: after each full scan, the spectra of the 10 highest-intensity parent ions were acquired; secondary MS resolution, 17,500 at m/z 200; AGC target, 1e5; and maximum IT, 50 ms. MS2 activation was HCD, with an isolation window of 2 m/z and stepped normalized collision energies of 20, 30, and 40 eV.

MS-DIAL was used to process the data, including peak alignment, retention time (Rt) correction, and peak area extraction. We used second-order spectral matching (mass tolerance <0.01 Da) and precise mass number matching (mass tolerance <20 ppm) to identify the metabolite structures after searching public databases such as HMDB, MassBank, and GNPS. We excluded the peak values of ions with more than 50% missing values. Then, we normalized and integrated the total peak areas from both positive and negative ion modes and applied Python software for pattern recognition. The data were then preprocessed using unit variance scaling. Variable importance in projection (VIP) values were derived from multivariate and univariate statistical analyses. Significant differentially abundant metabolites were identified on the basis of VIP>1 and P<0.05 from univariate analysis. KEGG pathway analysis was performed on the significantly differentially abundant metabolites selected, and the 30 pathways with the most significant differences were chosen and used to construct a significant pathway map to analyze the mechanism of action of SMW in reducing SUA levels.

Results

The Effect of SMW on SUA Levels in Hyperuricemic Rats

SUA levels were measured from the blood samples taken from the tail veins of the rats after 4 weeks of gavage; these results are presented in Figure 1. Compared with those in the model group, the SUA levels in the benzbromarone and high- and medium-dose SMW groups were significantly lower (P<0.01) and followed the order of benzbromarone (strongest effect), high-dose SMW, and medium-dose SMW (weakest effect).

Effects of SMW on the Liver Wet Weight and Liver Index in Hyperuricemic Rats

The hepatic index was calculated as the ratio of the liver wet weight to the rat body weight and it is an important index for assessing liver function. The liver wet weights, body weights, and hepatic indices of the rats in each group at the end of gavage treatment are given in Figure 2. As shown in Figure 2a and b, the liver index of the model group was slightly higher than that of the blank group; the liver index of the benzbromarone group was significantly greater than that of the blank group (P<0.01); and the liver indices of the medium- and low-dose SMW groups were lower than that of the benzbromarone group (P<0.05).

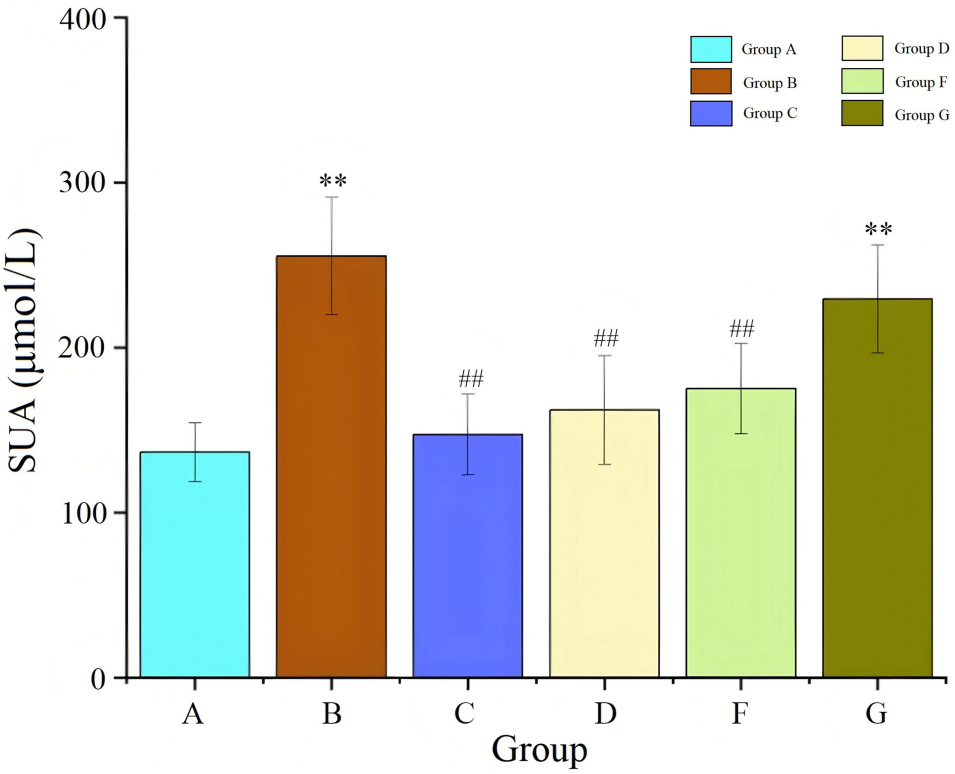

Figure 1 Effect of SMW on SUA levels in hyperuricemic rats (n=8). ** indicates a significant difference compared with blank group, P<0.01; ## indicates a significant difference compared with model group, P<0.01.

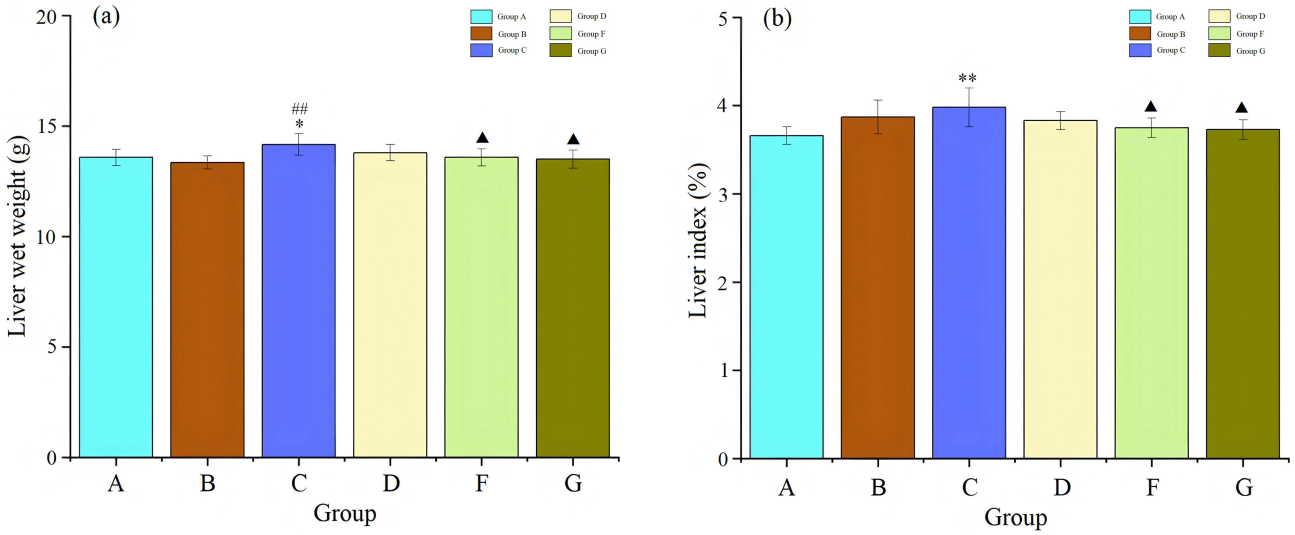

Figure 2 The liver wet weights (**a**) and liver index (**b**) of the rats in each group at the end of gavage treatment (n=8). * indicates a significant difference compared with the blank group, P<0.05; ** indicates a significant difference compared with the blank group, P<0.01; ## indicates a significant difference compared with the model group, P<0.01; ▲ indicates a significant difference compared with the benzbromarone group, P<0.05.

Effects of SMW on the Renal Wet Weight and Renal Index in Hyperuricemic Rats

The renal index was calculated as the ratio of the wet weight of both kidneys to rat body weight. When the kidneys are impaired, the renal index is elevated. As given in Figure 3a and b, compared with those of the blank group, the kidney wet weight of the model group was significantly greater (P<0.05) and the renal index was significantly greater (P<0.01).

https://doi.org/10.2147/DDDT.S533394

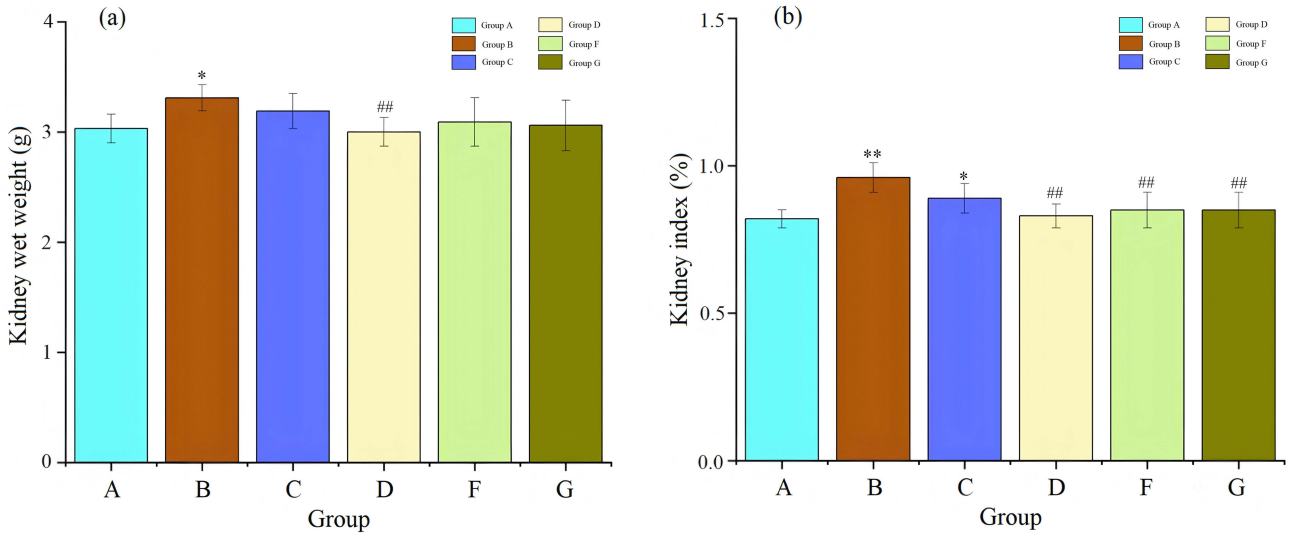

Figure 3 The kidney wet weights (**a**) and kidney index (**b**) of the rats in each group at the end of gavage treatment (n=8). *indicates a significant difference compared with the blank group, P<0.05; **indicates a significant difference compared with the blank group, P<0.01; ## indicates a significant difference compared with the model group, P<0.01.

Additionally, compared with that of the model group, the renal indices of the high-, medium-, and low-dose SMW groups were significantly lower (P<0.01).

Biochemical Indices

The levels ALT and AST in each group of rats after four weeks of gavage treatment are shown in Figure 4. As shown in Figure 4a and b, compared with those in the blank group, the serum levels of ALT and AST were elevated in the model group and especially in the benzbromarone group (P<0.01). Compared with those in the model group, the level of ALT in the benzbromarone group was significantly elevated, but the level of AST was not significantly different. Compared with those in the benzbromarone group, the ALT and AST levels were significantly lower in all SMW groups, especially in the SMW medium- and low-dose groups (P<0.05).

Effects of SMW on the Renal Function of Hyperuricemic Rats

BUN and serum CRE are important indicators of renal function. As shown in Figure 4c and d, the levels of BUN and CRE were significantly elevated in the model group compared with those in the blank group (P<0.01). Moreover, compared with those in the model group, the levels of BUN and CRE were reduced to different degrees in the benzbromarone and SMW groups, among which the serum BUN levels were significantly reduced in the high-, medium-, and low-dose SMW groups (P<0.05) and the serum CRE levels were significantly reduced in the medium- and low-dose SMW groups (P<0.01).

Metabolomics

Quality Evaluation

The QC samples were prepared and subjected to MS and principal component analysis (PCA) to evaluate the stability of the experimental system. Figure 5a and b presents the total ion chromatograms (base peaks) of the QC sample mass spectra in positive and negative ion modes, respectively. The intensities and retention times (Rt) of the peaks were largely consistent, indicating that minimal instrumental error occurred during the experiment and confirming the reliability of the data. In the figure, the horizontal axis represents the Rt of the metabolite in the chromatogram, whereas the vertical axis indicates the ion intensity. As shown in Figure 5, the QC samples tightly clustered together, indicating excellent repeatability of the experiments. In conclusion, the instrumental analysis system demonstrated good stability, and the

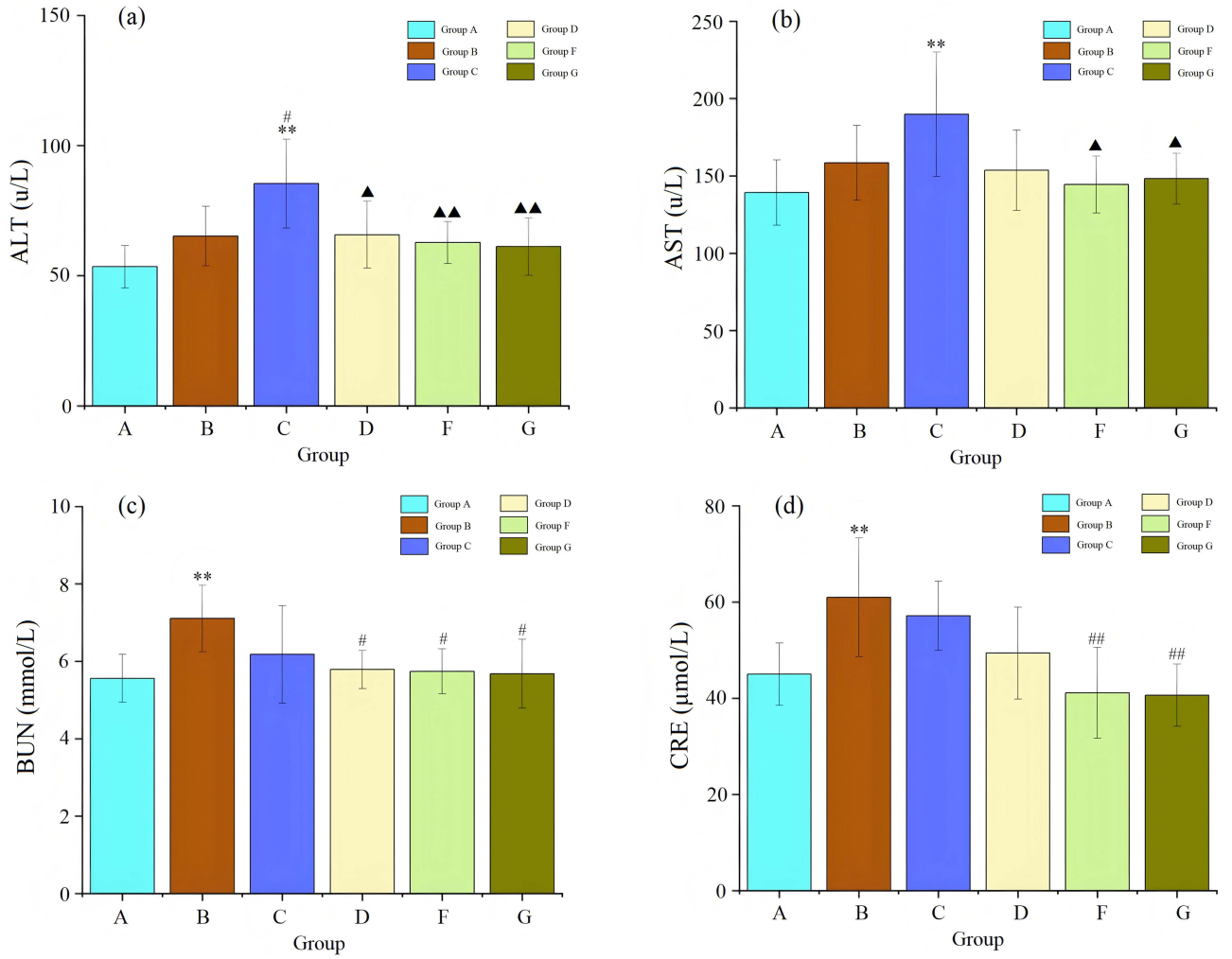

Figure 4 The levels ALT (**a**) AST (**b**) BUN (**c**), and CRE (**d**) in each group of rats after four weeks of gavage treatment (n=8). ** indicate a significant difference compared with the blank group, *P*<0.01; # indicates a significant difference compared with the model group, P<0.05; ## indicates a significant difference compared with the model group, P<0.01; ▲ indicates a significant difference compared with the benzbromarone group, P<0.05; ▲▲ indicates a significant difference compared with the benzbromarone group, P<0.01.

experimental data were stable and reliable. Thus, the differences in the detected metabolic profiles reflect the biological variations among the samples.

We extracted the metabolite ion peaks using MS-DIAL software, and 11981 peaks were obtained in positive mode and 12943 peaks were obtained in negative mode. The peaks extracted from the QC samples and all test samples were processed by UV and then subjected to PCA. The PCA model obtained after 7 cross-validation cycles is shown in Figure 6a. Additionally, Figure 6b depicts the 3D PCA score plot of the QC samples.

Statistical Analysis of the Significantly Differentially Abundant Metabolites

One-way ANOVA was used to assess the significance of the differentially abundant metabolites across multiple groups. Metabolites with P<0.05 and an orthogonal projections to latent structures-discriminant analysis (OPLS-DA) VIP>1 were considered significantly different. Overall, upon comparison of groups A, B, and F in positive ion mode (POS), negative ion mode (NEG), and integrated mode (MIX, which is the sum of the positive and negative values after duplicate removal), were 91, 154, and 245 differentially abundant metabolites were identified, respectively.

https://doi.org/10.2147/DDDT.S533394

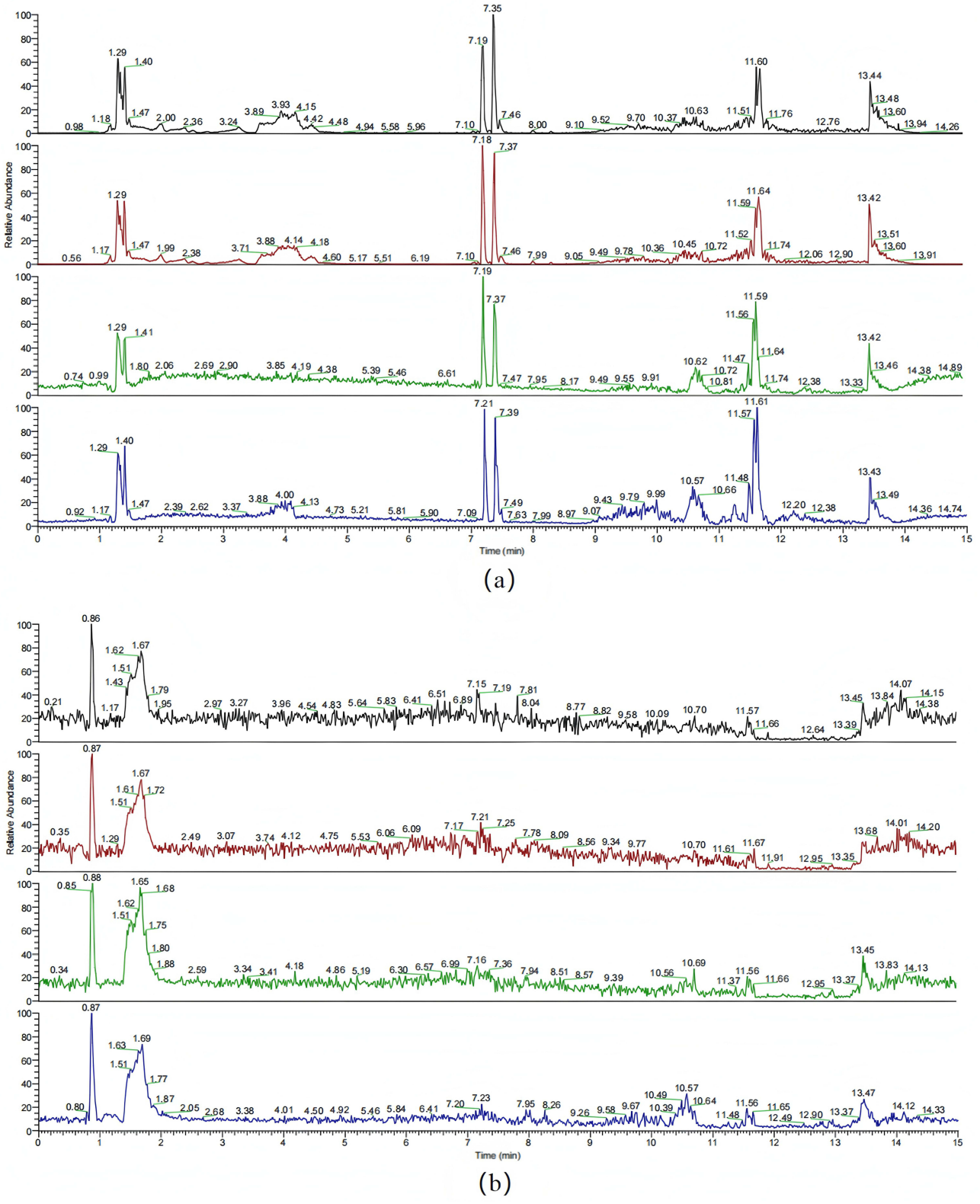

Figure 5 The base peak spectrum of the QC sample in positive ion mode (**a**) and in negative ion mode (**b**). Among the four different color chromatograms, one color represents a single detection of the QC sample.

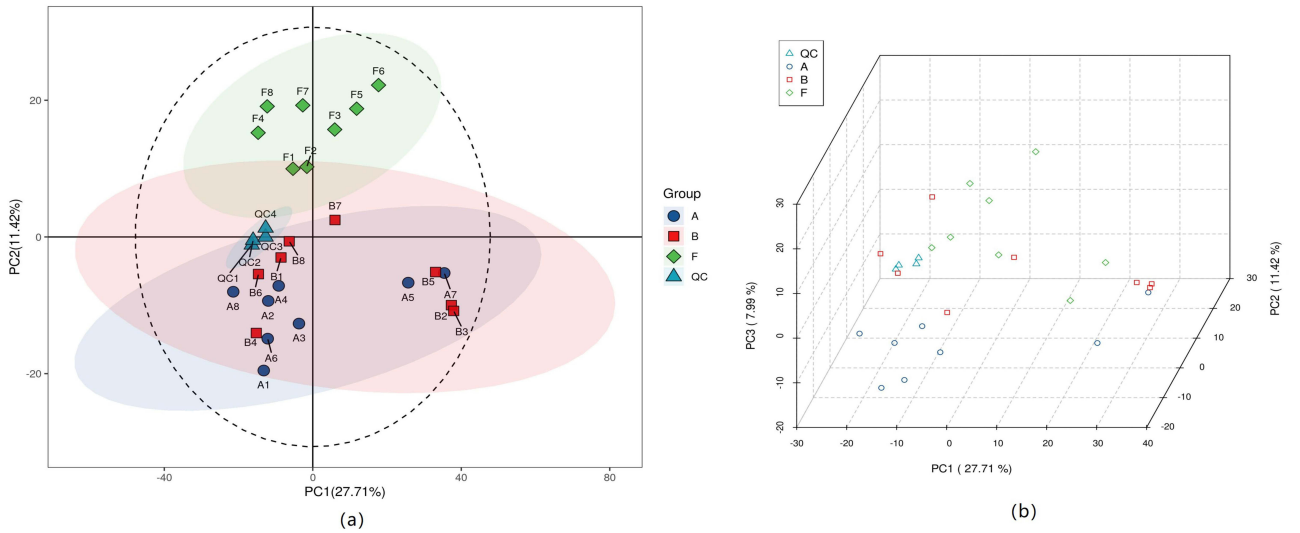

Figure 6 The PCA score plot of the QC samples (**a**) and the three-dimensional PCA score plot of the QC samples (**b**). Group (A) blank; Group (B) HUA model; Group (F) Medium-dose SMW.

PCA

We conducted PCA of the metabolites to gain a preliminary understanding of the differences among the sample groups and the degree of variability within each group. The parameters of the PCA model for groups A, B, and F were R2X (cum, 0.536, indicating the explanation rate of the model) and Q2 (cum, 1.062, indicating the predictive ability of the model). The PCA score plots are shown in Figure 7a.

The presence of many endogenous metabolites in the blood and their complex compositions lead to high noise levels during analysis. Since PCA is an unsupervised mode of analysis and thus not ideal for classification and identification, we applied the supervised discriminant analysis method partial least squares-discriminant analysis (PLS-DA), for more precise classification.

PLS-DA

PLS-DA is a supervised discriminant analysis method that employs partial least squares regression to model the relationship between sample categories and metabolite expression, allowing for the prediction of sample categories. We built PLS-DA models for each comparison group A, B, and F, and the evaluation parameters of the models were as follows: R2X (cum, 0.119), R2Y (cum, 0.691), and Q2 (cum, 0.312). The scores of the models are shown the plots in Figure 7b, and the closer R2 and Q2 are to 1, the more stable and reliable the model is; additionally, Q2 was greater than 0.5, which indicates that the model's prediction ability is good.

OPLS-DA

On the basis of PLS-DA, this method was used to filter out noise to greatly improve the analytical capacity and validity of the model. The OPLS-DA VIP values were calculated to assess how the expression pattern of each metabolite influences categorical discrimination among sample groups. Metabolites with a VIP value greater than 1.00 were considered significantly differently abundant. The evaluation parameters of the OPLS-DA model established for each comparison group A, B, and F (POS+NEG) were R2X (cum, 0.445), R2Y (cum, 0.983), and Q2 (cum, 0.819). The model score plot is shown in Figure 7c.

Permutation Test

To verify the reliability of the supervised classification model, in addition to internal validation (cross-validation), we can also apply a permutation test for external validation.

Figure 8 shows the validation of the PLS-DA and OPLS-DA models for groups A, B, and F, respectively, ie, the permutation test plots. After 200 permutation tests, the data were plotted wherein the horizontal axis represents the

https://doi.org/10.2147/DDDT.S533394

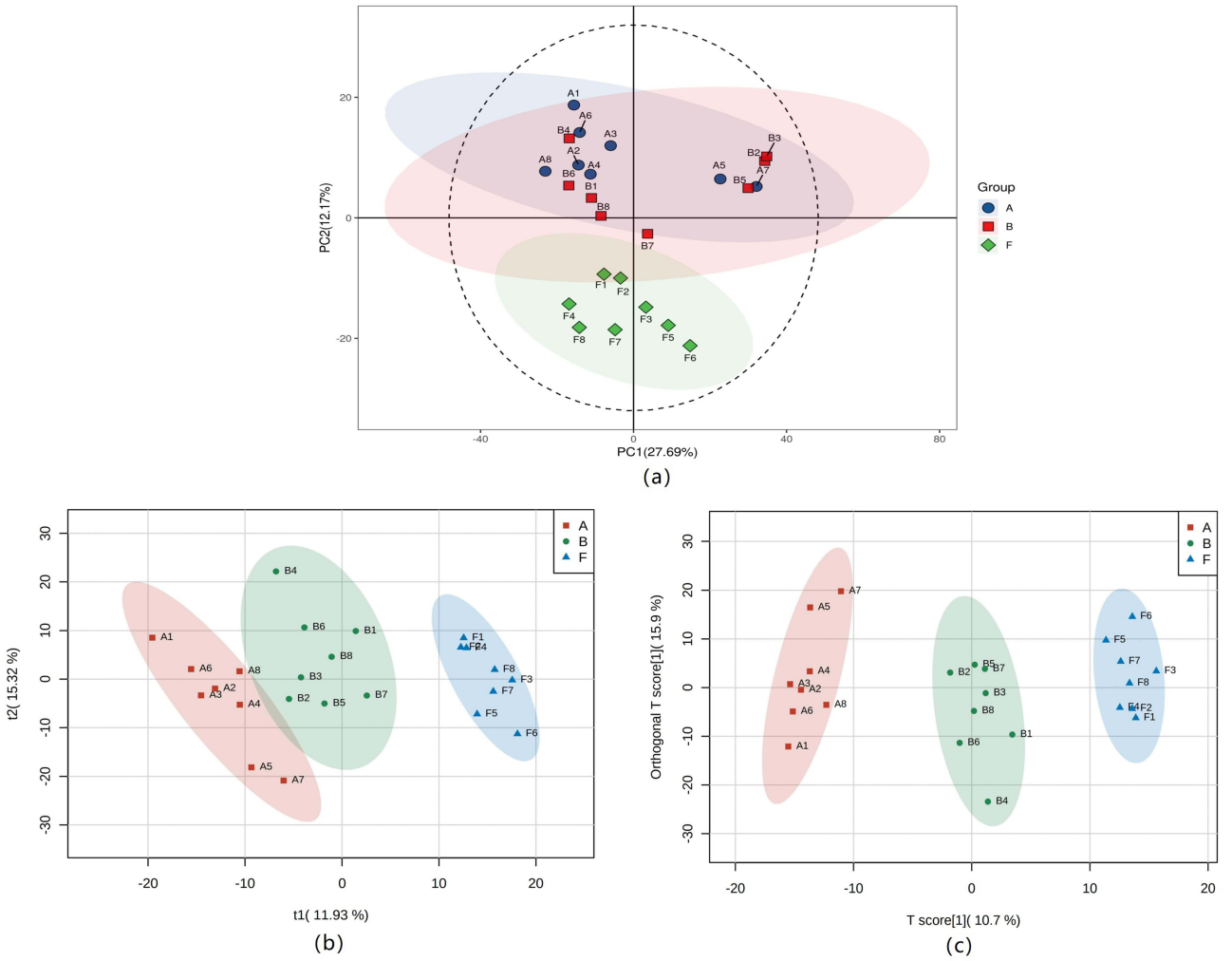

Figure 7 The PCA score plots of groups A, B, and F in positive and negative ion modes (**a**), the PLS-DA score plots of groups A, B, and F in positive and negative ion modes (**b**) and the OPLS-DA score plots of groups A, B, and F in positive and negative ion modes (**c**).

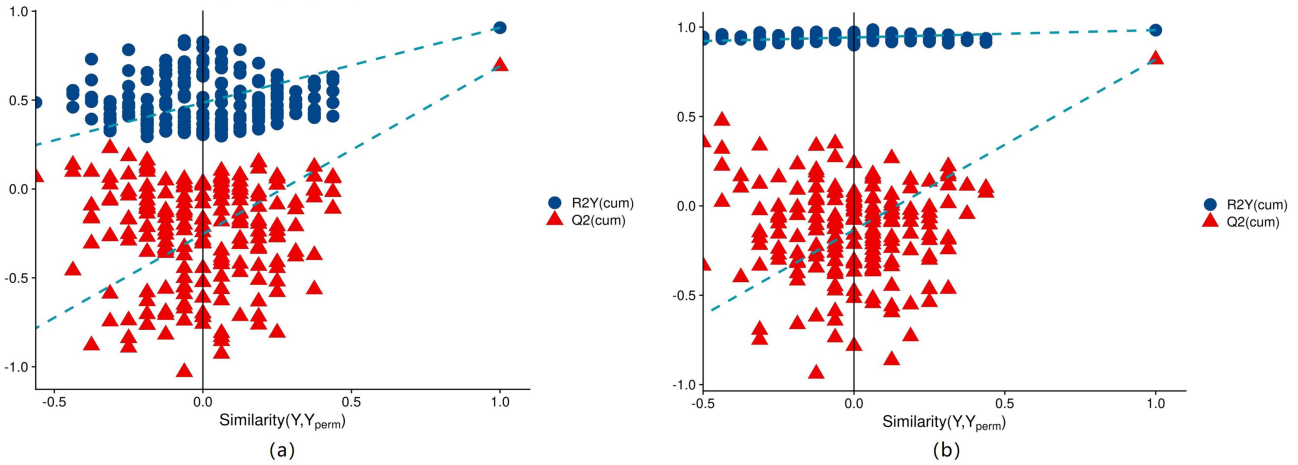

Figure 8 The OPLS-DA permutation test plot with R_2 (0, 0.4849) and Q_2 (0, −0.25) for comparison of groups A, B, and F (**a**) and the OPLS-DA permutation test plot with R_2 (0, 0.9423) and Q_2 (0, −0.13) for comparison of groups A, B, and F (**b**).

correlation between the Y values of the random group and the Y values of the original group, and the vertical axis represents the R2 and Q2 scores. The quality of the multivariate statistical analysis model was ultimately assessed on the basis of the permutation test results. The model is considered highly reliable if either the Y-intercept of the Q2 regression line is less than zero or if the Q2 scores from the 200 permutation tests are lower than those of the original model. The Y-intercept of the Q2 regression line suggests that the model did not fit the experimental data, which indicates that there are indeed differences between the groups of plasma samples, and further analysis of the variation in these differences is necessary.

Univariate Statistical Analysis

The lower panels of Figure 9 show the volcano plots of the comparison groups for which P values were obtained using Student's *t* test. The identified metabolites were categorized on the basis of the KEGG results and are represented by different colors and shapes. P<0.05 and a fold change (FC) of >1.5 or <1/1.5 were used as the screening criteria. The

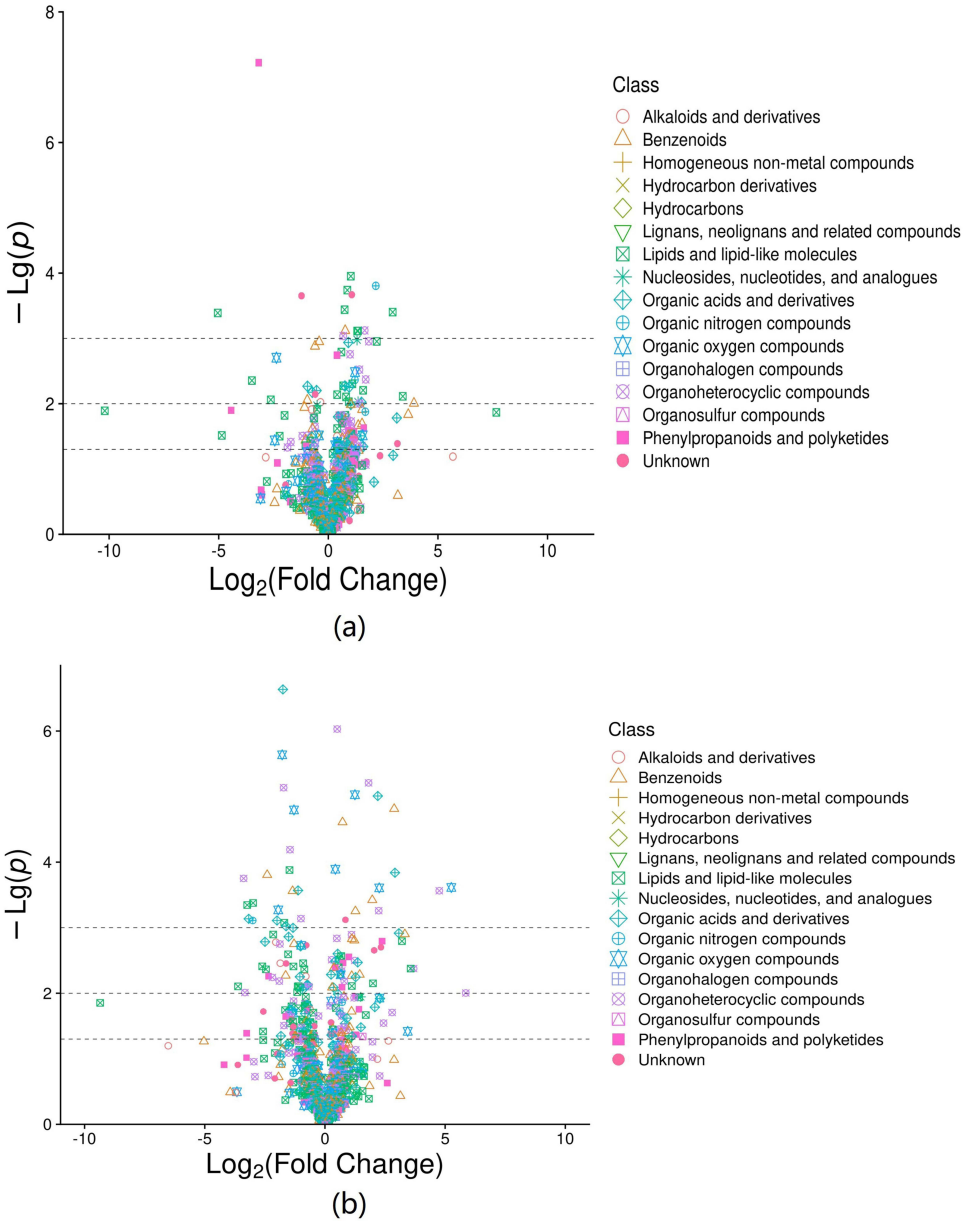

Figure 9 The volcano plot of the ion patterns in positive and negative modes for the A vs B comparison group (**a**) and the volcano plot of the ion patterns in positive and negative modes for the B vs F comparison group (**b**). The three horizontal lines represent p-values: 0.001 (top), 0.01 (middle), and 0.05 (bottom).

https://doi.org/10.2147/DDDT.S533394

vertical dashed lines are located at log2(1/1.5) and log2(1.5), and the increased differentially abundant metabolites (determined by univariate statistical analyses) are indicated by red dots, while the decreased differentially abundant metabolites are indicated by blue dots.

Significantly Differentially Abundant Metabolites

In this study, a VIP value greater than 1 was used as the criterion for screening metabolites and served as the initial condition to identify differences among the groups. The metabolites with VIP>1 according to multivariate statistical analysis and P<0.05 according to univariate statistical analysis were identified as significantly differentially abundant. After integrating the data from all the groups, we identified a total of 131 metabolites with significantly different abundances between group A and group B. Among them, 47 metabolites were detected in positive ion mode, with 24 increased metabolites and 23 decreased metabolites; and 84 metabolites were detected in negative ion mode, with 65 increased metabolites and 19 decreased metabolites. The four significant differential metabolites among groups A and B are shown in Table 1. At the same time, we identified a total of 212 significantly differentially abundant metabolites in the group B and group F comparison. Among them, 64 metabolites were detected in positive ion mode, with 21 increased metabolites and 43 decreased metabolites; and 148 metabolites detected in negative ion mode, with 76 increased metabolites and 72 decreased metabolites. The four significant differential metabolites among groups B and F are shown in Table 2.

In this study, metabolites with VIP>1.0 and 0.05<0.1 were not examined, only the significantly differentially abundant metabolites were analyzed.

Bioinformatics Analysis

KEGG pathway analysis can provide a more comprehensive understanding of cellular biological processes, traits, or mechanisms of disease occurrence. Such an analysis will enhance our understanding of metabolite functions and their relationships. Therefore, the significantly differentially abundant metabolites between groups A and B, B and F, and A and F were subjected to KEGG analysis, and the 30 most significant different pathways were selected to generate KEGG pathway enrichment bubble maps (see Figure 10).

By analyzing the enriched KEGG pathways for the A and B, B and F, and A and F comparison groups, the effects of HUA on metabolism, the possible mechanism of action of SMW in lowering SUA levels, and the potential of using SMW in the treatment of other diseases can be determined.

From the AB group comparison (Figure 10a), the effect of HUA on metabolism can be determined, which can be used to understand the effects of HUA on metabolite expression and provide directions for the treatment of HUA.

The therapeutic effect of SMW on HUA was reflected in the BF group comparison (Figure 10b). Furthermore, the identified KEGG metabolic pathways could reflect how SMW affects the expression of metabolites in hyperuricemic model rats to a certain extent.

Table 1 The Four Significant Differential Metabolites Among Groups A and B

KEGGID	AlignmentID	Metabolite Name	Formula	VIP value	P.value	Rt (min)	FC
C00407	POS1624	L-Isoleucine	C6H13NO2	2.082913582	0.006290132	7.406	0.6893226
C00208	POS6829	(S)-maltose	C12H22O11	1.761357569	0.03059504	1.315	0.7423405
C00158	NEG2238	Citrate	C6H5O7	2.218680205	0.000145117	3.371	7.528270715
C00624	POS3526	N-acetyl-L-glutamic acid	C7H11NO5	1.732951185	0.032480786	8.979	0.5932076

Table 2 The Four Significant Differential Metabolites Among Groups B and F

KEGGID	AlignmentID	Metabolite Name	Formula	VIP value	P.value	Rt (min)	FC
C00158	NEG2238	Citrate	C6H5O7	2.218680205	0.000145117	3.371	7.528270715
C00135	NEG1329	L-histidine	C6H9N3O2	1.84510418	0.005203619	0.827	1.193187078
C00062	NEG1836	L-arginine	C6H14N4O2	1.782647571	0.008168497	0.842	1.277782339
C01468	POS327	4-Cresol	C7H8O	2.15917886	0.000275524	8.302	0.393312792

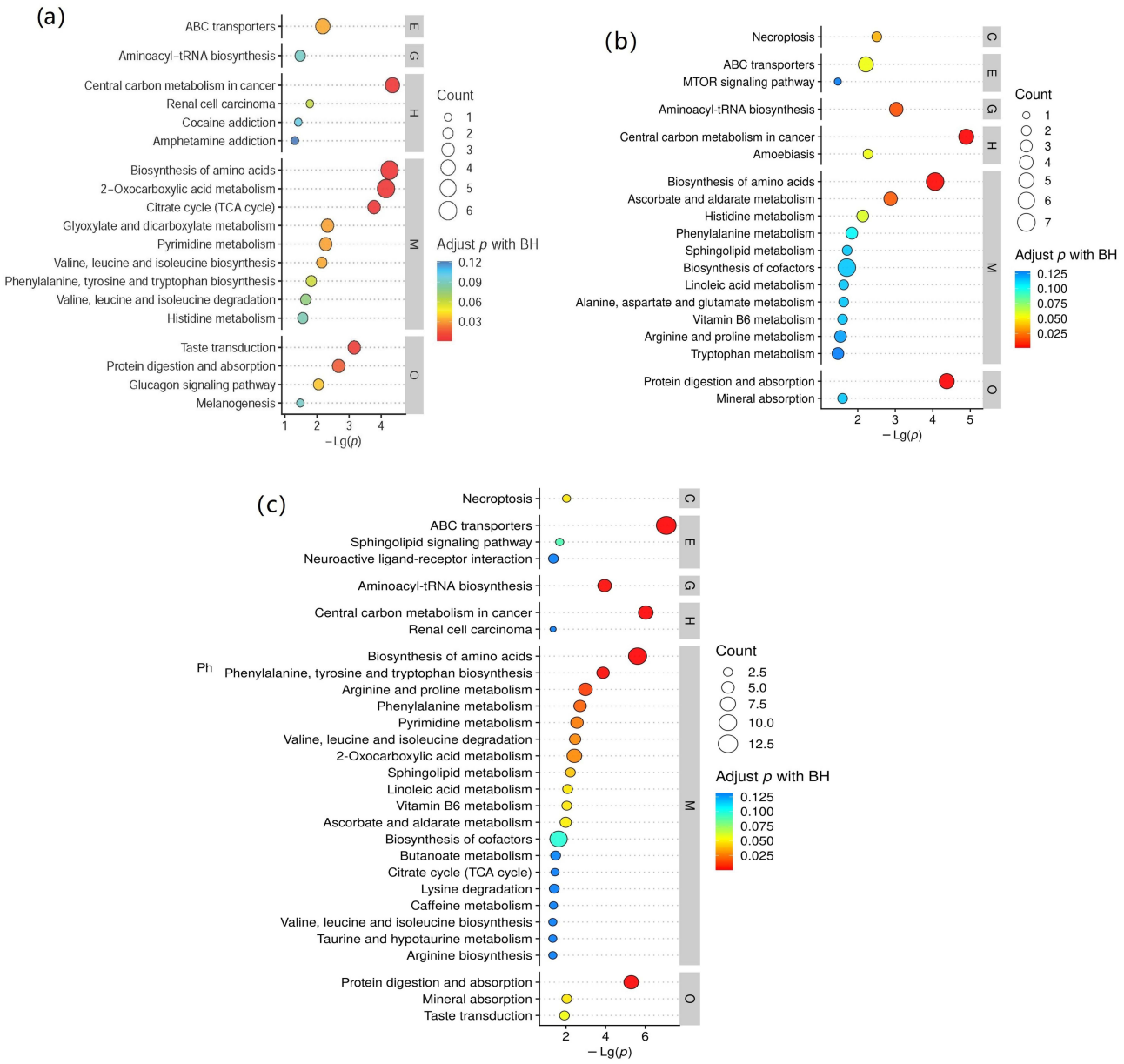

Figure 10 The KEGG pathway enrichment analysis of the significantly differentially abundant metabolites between groups A and B (**a**), between groups B and F (**b**) and between groups A and F (**c**).

The AF group comparison (Figure 10c) represented how SMW affects metabolism under normal conditions. This finding reflects, to a certain extent, the pathways specifically involved in the active ingredients in SMW, as well as the potential therapeutic effects of SMW on other diseases.

In summary, the potential association between SMW and HUA can be understood through the KEGG AB, BF, and AF intergroup comparisons. These findings can help us to better understand how SMW affects metabolism under different conditions and provide a reference for the study of related diseases.

The bubble diagram of the AB comparison group revealed three very important pathways, listed from high to low significance: central carbon metabolism in cancer, biosynthesis of amino acids, and 2-oxocarboxylic acid metabolism.

The bubble diagram of the BF comparison group revealed three important pathways, listed in descending order of significance: central carbon metabolism in cancer, protein digestion and absorption, and the biosynthesis of amino acids,

https://doi.org/10.2147/DDDT.S533394

Table 3 Notable Pathways and Their Enriched Differentially Abundant Metabolites for the A and B Group Comparison

Pathway	Number of Differentially Abundant Metabolites	Differentially Abundant Metabolites
Central carbon metabolism in cancer	4	L-Isoleucine, (S)-maltose, L-tyrosine, citrate
Protein digestion and absorption	6	3-Dehydroquinoline, 4-methyl-2-oxovaleric acid, L-isoleucine, N-acetyl-L-glutamic acid, L-tyrosine, citrate
2-Oxocarboxylic acid metabolism	6	4-Methyl-2-oxovaleric acid, L-isoleucine, cis-aconitate, N-acetyl-L-glutamic acid, L-tyrosine, citrate

Table 4 Notable Pathways and Their Enriched Differentially Abundant Metabolites for the B and F Group Comparison

Pathway	Number of Differentially Abundant Metabolites	Differentially Abundant Metabolites
Central carbon metabolism in cancer	5	Citrate, L-histidine, L-arginine, L-alanine, L-methionine
Protein digestion and absorption	5	4-Cresol, L-histidine, L-arginine, L-alanine, L-methionine
Biosynthesis of amino acids	7	Citrate, L-histidine, 4-methyl-2-oxovalerate, L-arginine, D-erythrose-4-phosphate, L-alanine, L-methionine

among which the most significantly enriched differentially abundant metabolite was associated with the biosynthesis of amino acids.

We identified the significantly differentially abundant metabolites enriched within the central carbon metabolism in cancer pathway via KEGG plots. Additionally, Tables 3 and 4 show the significant pathways enriched in the differentially abundant metabolites in the AB and BF group comparisons, respectively.

Discussion

Effects of SMW on Lowering UA Levels and Hepatic and Renal Function

UA Lowering Effect of SMW

In the animal experiments, we used 12% yeast paste combined with 2% potassium oxonate to establish a rat model of HUA. Potassium oxonate is a uricase inhibitor that that competes with UA binding, which causes this enzyme to lose its biological activity. Additionally, yeast causes the contents of UA precursors to increase in vivo. Thus, this dual agent model allows bidirectional promotion of sustained increases in UA levels in rats and effectively simulates high purine diet-induced HUA in humans.[6,7]

SMW contains a variety of active ingredients, such as the typical flavonoid quercetin, which is the main component of Huang Bai and Niu Xi. Quercetin reduces the level of UA and protects the kidneys by regulating the expression levels of uromodulin and renal organic ion transporter proteins.[8] Berberine exhibits anti-inflammatory activity primarily by inhibiting the PI3K/AKT signaling pathway, which reduces the levels of serum proinflammatory factors such as tumor necrosis factor α (TNF-α), interleukin 1β (IL-1β), and IL-6.[9] In addition, quercetin and baicalein can reduce SUA levels by inhibiting xanthine oxidase activity in hyperuricemic rats.[10]

Effects of SMW on Liver Function in Hyperuricemic Rat Models

ALT and AST are commonly used indicators of liver function. When liver cells in the body are damaged, intracellular aminotransferases enter the bloodstream, causing elevated serum ALT and AST concentrations. Therefore, aminotransferases are sensitive markers of hepatocellular injury and an important basis for determining liver injury. Compared with those in the blank group, the serum ALT and AST levels were elevated in both the model group and the benzbromarone group, with the benzbromarone group showing a particularly significant increase ($P<0.01$). Compared with that in the model group, the ALT level in the benzbromarone group was significantly elevated, indicating that benzbromarone may have a detrimental effect on liver function. Compared with those in the benzbromarone group, the ALT and AST levels in

all the SMW groups (especially the medium- and low-dose SMW groups) were significantly lower ($P<0.05$), indicating that SMW can protect liver function by reducing the SUA concentration.

The hepatic index was calculated as the ratio of the wet weight of the rat liver to the body weight. When liver cells are damaged, the liver volume and weight increase, and thus, the liver index increases. Therefore, the liver index is considered an important indicator of liver function. Compared with that of the blank group, the liver index of the model group was slightly elevated, suggesting that some inflammation occurred in the liver following modeling. The hepatic index of the benzbromarone group was significantly greater than that of the blank group ($P<0.01$), indicating that benzbromarone caused liver damage. The liver indices of the medium- and low-dose SMW groups were lower than those of the benzbromarone group ($P<0.05$), indicating that SMW protected the liver while lowering blood UA levels.

Pathological changes, such as the hydropic degeneration of hepatocytes around the central vein and the swelling of hepatocytes in the liver tissue of the benzbromarone group, were observed in the pathological liver sections from all the groups, whereas no inflammatory reactions were observed in the high-, medium-, and low-dose SMW groups, and the hepatocytes tended to appear normal. These pathological results confirmed the hepatoprotective effects of SMW.

Recent studies from around the world have proposed that the mechanism of benzbromarone-mediated liver injury could include metabolite toxicity and mitochondrial toxicity. Benzbromarone interferes with the normal function of the mitochondria, and confocal microscopy and transmission electron microscopy revealed that benzbromarone may induce apoptosis by affecting the mitochondrial structure.[11] The hepatotoxicity of CYP450 metabolites of benzbromarone, such as 2,6-dibromohydroquinone, 2-ethyl-3-(3-bromo-4,5-dihydroxybenzoyl) benzofuran, 1,6-dihydroxybenzbromarone, and 6-epoxy benzbromarone, has been demonstrated in vitro in several studies.[12,13]

Effects of SMW on Renal Function in Hyperuricemic Model Rats

BUN is the end product of amino acids that undergo the ornithine cycle in the liver and is excreted in the urine after glomerular filtration, with approximately 60% of the urea being reabsorbed by the proximal tubules of the kidneys. Therefore, when kidney function is impaired, urea glomerular filtration is reduced, and the concentration of urea in the blood increases. CRE is the final metabolite of muscles that is also excreted via glomerular filtration. CRE is largely filtered through the glomerulus and is not reabsorbed. When muscle metabolism is relatively stable, CRE production is essentially constant. However, when renal function is severely impaired, the serum CRE and BUN levels are significantly elevated. Therefore, increases in the BUN and CRE concentrations can be used to evaluate renal function impairment.

Compared with those in the blank group, the BUN and CRE levels were significantly elevated in the model group ($P<0.01$), suggesting that the sustained increase in SUA concentration led to renal function damage. Compared with those in the model group, the BUN and CRE levels were reduced to varying degrees in the benzbromarone and SMW groups, among which the serum BUN level was significantly lower in the high-, medium- and low-dose SMW groups ($P<0.05$), and the serum CRE level was significantly lower in the medium- and low-dose SMW groups ($P<0.01$). These findings indicate that benzbromarone and SMW alleviate renal function damage caused by HUA by reducing the SUA concentration and that SMW protects the kidneys better than the positive control drug benzbromarone does.

The renal index was calculated as the ratio of the wet weight of both kidneys to the body weight. When the kidneys are impaired, the weight of the kidneys increases, as does the renal index. Therefore, the renal index is considered an important indicator of renal function. Compared with the blank group, the model group presented a significantly greater renal wet weight ($P<0.05$) and renal index ($P<0.01$), suggesting that the sustained increase in SUA levels in the model group damaged renal function. Compared with those in the model group, the renal indices were significantly lower in the high-, medium- and low-dose SMW groups ($P<0.01$). This finding also indicated that SMW improved the renal impairment caused by HUA by lowering SUA levels and that SMW had a better renoprotective effect than the positive control drug benzbromarone did.

Pathological changes in the renal tissues of the hyperuricemic model group, such as tubular atrophy, decreased volume, increased cytoplasmic basophilicity of tubular epithelial cells, and tubular dilatation, were observed in the kidney sections of the rats in each group. Compared with the model group, the benzbromarone group presented pathological damage to a lesser extent. Compared with those of the model group and the benzbromarone group, all the SMW groups presented improvements, as the structures of the renal microsomes were clear, and no obvious damage

was observed. The pathologic results confirmed that SMW alleviated renal impairment due to HUA while lowering the SUA level.

HUA has a direct pathogenic effect on the kidneys. When the SUA concentration in patients with HUA is persistently high, urate crystals can precipitate and be deposited in the kidneys, causing tubular obstruction, which can lead to renal injury, eg, hyperuricemic nephropathy or gouty nephropathy. The typical pathological feature of renal injury caused by HUA is an inflammatory response. High SUA levels promote the secretion of large amounts of inflammatory factors (eg, interleukins, colony-stimulating factor, and tumor necrosis factor) and chemokines by damaged renal tubular epithelial cells, which results in the aggregation of many inflammatory cells at the site of injury.[14]

From the above experimental data, we concluded that SMW significantly reduced the blood UA concentration in rats, and the UA lowering effects of the high and middle doses of SMW were similar to that of the positive control drug benzbromarone. Moreover, in addition to lowering blood UA levels, SMW reduced the damage to renal function caused by HUA, and increased ALT and AST levels noted in the livers of the benzbromarone group were not detected in the high-, medium- and low-dose SMW groups. SMW alleviated renal function injury due to HUA in rats by lowering the SUA concentration, and its liver protective effect was better than that of benzbromarone. The protective effects of SMW on liver and kidney function in hyperuricemic model rats was demonstrated throughout the entire treatment process.

Metabolomics Analysis of the SMW-Mediated Reduction in SUA Levels

Metabolomics analysis showed that the significantly altered metabolic pathways in the AB comparison group were central carbon metabolism in cancer, biosynthesis of amino acids, and 2-oxocarboxylic acid metabolism. The differentially abundant metabolites within these pathways were dominated by various amino acids and citrate (of which citrate was enriched in all three pathways), suggesting that the above differentially abundant metabolites were perturbed when the blood UA concentration increased.

The notable metabolic pathways enriched in the differentially abundant metabolites in the BF comparison group were central carbon metabolism in cancer, protein digestion and absorption, and biosynthesis of amino acids. These three pathways included most of the significantly differentially abundant metabolites in the KEGG pathway, indicating that the possible mechanism of action of SMW in lowering SUA concentrations was related to these three pathways.

Citrate (C00158)

Citrate is an intermediate product in the metabolism of sugars, lipids, and certain amino acids in living organisms and plays crucial roles in both material and energy metabolism. An important step in the oxidative decomposition of these three types of substances is the generation of coenzyme acetate, which is catalyzed by citrate synthase and also produces citrate. This step is the first in the tricarboxylic acid cycle (also known as the citric acid cycle). Citrate is the strongest inhibitor of endogenous stone formation in urine and has certain pharmacological effects, such as urine alkalinization, the prevention and treatment of calcium-containing kidney stones, metabolic acidosis treatment, and gastric acid neutralization. Medications commonly used in clinical practice that contain citrate include potassium citrate and sodium citrate preparations.[15] It has been proven that potassium citrate and sodium acetate are metabolized to carbonate oxygenates via the tricarboxylic acid cycle, which increases the concentration of carbonate oxygenates in the blood and urine and thus promotes the excretion of UA and other metabolically disturbed acids to alleviate the symptoms of gout, HUA and acidosis, etc. Moreover, another study showed that potassium citrate, an alkalizing agent and potassium supplement, can lead to alkaline load in the body, promote urinary citrate excretion, and inhibit the formation of UA crystals and calcium oxalate stones.[16] This is because after potassium citrate is oxidized in the body, potassium ions form an alkaline load, leading to elevated urinary pH, which in turn increases UA solubility. The levels of urinary citrate ions increase, these citrate ions can compete with oxalate ions for calcium ion binding to form water soluble calcium citrate complexes, which promote the elimination of calcium in the urine. Moreover, potassium citrate can also decrease calcium secretion in the urine, reduce the formation of calcium crystals, and promote the gradual dissolution of already formed calcium crystals.[17]

HUA is an independent risk factor for kidney stone formation. If blood UA levels continue to rise, large amounts of urate will be deposited in the interstitium of the renal tubules to form stones and cause local chemical inflammation. These deposits may even lead to renal tissue atrophy and fibrous degeneration, causing sclerosis of the small renal

arteries and glomeruli and ultimately leading to renal failure. Citrate ions can promote UA excretion, inhibit urate crystallization, and improve the symptoms of HUA. In this study, citrate metabolism was activated in the hyperuricemic rat model after gavage with SMW, suggesting that SMW may play a role in lowering the SUA concentration while also protecting the kidneys by increasing citrate metabolism.

L-Histidine (C00135)

Histidine is an essential amino acid for humans and other mammals. Studies have shown that L-histidine can scavenge the reactive oxygen species (ROS) produced by cells during the acute inflammatory response, inhibit the expression of proinflammatory factors involved in tissue damage, and exert anti-inflammatory and antioxidative effects.[18] The protective mechanism by which histidine plays an important role in antioxidant defense is its direct scavenging of ROS produced by cells during acute inflammatory responses through its imidazole ring. In addition, iron, copper, nickel, chromium, and zinc ions can be toxic to organisms by promoting the production of free radicals through the Fenton reaction, whereas histidine can reduce the ROS production by chelating the above metal ions.[19,20] Experiments have been conducted to detect ROS levels and apoptosis-related indicators in liver cells after liver ischemia–reperfusion and to investigate the mechanism by which histidine improves liver cell injury and apoptosis caused by liver ischemia–reperfusion. Compared with those in the negative control cells, the ROS levels in the hypoxia/reoxygenation THLE cells were significantly greater. An increase in ROS levels can increase the levels of apoptosis-related factors, whereas histidine treatment significantly reduces ROS levels in cells. Furthermore, treatment with histidine significantly reduced the levels of proapoptotic proteins such as Bax and Bcl-2 in liver tissue while increasing the levels of antiapoptotic proteins. Thus, histidine inhibits liver cell apoptosis and improves liver tissue ischemia–reperfusion injury by reducing cellular ROS levels.[21]

The anti-inflammatory and antioxidant effects of L-histidine are achieved mainly through the NF-κB and PPARγ pathways. C-reactive protein, IL-6, and TNF-α promote the inflammatory response. NF-κB is a key transcription factor for inflammatory response genes and stimulates the synthesis of these factors. L-Histidine can exert anti-inflammatory effects by inhibiting NF-κB activation and decreasing the production of proinflammatory cytokines. HUA is a metabolic disease that incorporates inflammatory and oxidative stress (OS) reactions. Therefore, SMW exerts anti-inflammatory and antioxidant effects by increasing L-histidine metabolism in the treatment of HUA.

L-Arginine (C00062)

L-Arginine is a functional amino acid that plays crucial roles in the body's physiological functions, metabolism, and nutrition. The active form of arginine is L-arginine. The accumulation of free radicals can lead to OS, which in turn can cause various diseases. Research has shown that arginine has antioxidant effects, as it can increase the expression of endogenous antioxidant enzymes in rats, promote glutathione (GSH) synthesis, reduce the production and accumulation of ROS, increase the levels of antioxidants in the body, and mitigate OS.[22] Dasgupta et al reported that arginine supplementation can significantly increase the production of metabolic products, reduce lipid peroxidation in the body, increase the activities of endogenous antioxidant enzymes such as superoxide dismutase (SOD), catalase (CAT), and glutathione peroxidase (GPx), and reduce OS in a sickle cell anemia mouse model.[23] Arginine can effectively inhibit the oxidative degradation of myofibrillar protein structure and promote the formation of enhanced gel properties.[24]

Finally, as a metabolic byproduct of living organisms, UA, at normal physiological levels, has important roles. UA is a major antioxidant that ensures the health of the immune system, protects the brain and central nervous system, maintains vascular elasticity, controls blood pressure, and maintains stable bone density.[25] However, under the action of the antioxidant transport mechanism, the antioxidant properties of UA may be altered, leading to OS and inflammatory reactions. Research has confirmed that UA can cause damage to kidneys by activating the RAS system, promoting fibrosis, damaging the renal arterioles, affecting glomerular podocyte function, fostering proteinuria, and triggering OS and inflammatory reactions.[26] Among mechanisms, SOD plays a key role as the primary intracellular antioxidant defense factor.

In this study, the hyperuricemic model rats presented a significant decrease in SUA levels after treatment with SMW. Through metabolomics analysis, it was determined that SMW affects central carbon metabolism in cancer, protein digestion and absorption, and amino acid biosynthesis pathways while lowering SUA levels. Citrate was identified in the above pathways and can promote the excretion of UA and other metabolically disturbed acids, whereas citrate, L-histidine, and

L-arginine all have antioxidant and anti-inflammatory effects. The concentrations of these metabolites increased after treatment with SMW. Finally, it was concluded that the aforementioned metabolites play crucial roles in lowering SUA levels and in the protective effects of SMW on the liver and kidneys.

Conclusions

SMW effectively reduced the SUA level in a hyperuricemic rat model and alleviated the renal impairment induced by HUA in rats. Protective effects on liver and kidney function were demonstrated in the hyperuricemic model rats throughout treatment. The potential mechanism by which SMW lowers SUA levels is closely related to pathways such as central carbon metabolism in cancer, protein digestion and absorption, and the biosynthesis of amino acids.

Data Sharing Statement

All data generated in the present study may be requested from the corresponding author Xiangjun Qiu by Email lyxiangjun@126.com.

Author Contributions

All authors made a significant contribution to the work reported, whether that is in the conception, study design, execution, acquisition of data, analysis and interpretation, or in all these areas; took part in drafting, revising or critically reviewing the article; gave final approval of the version to be published; have agreed on the journal to which the article has been submitted; and agree to be accountable for all aspects of the work.

Funding

Special Project for Traditional Chinese Medicine Scientific Research in Henan Province in 2023 (2023ZY2130).

Disclosure

The authors declare that they have no conflicts of interest.

References

1. Chen PH, Chen YW, Liu WJ, Hsu SW, Chen CH, Lee CL. Approximate mortality risks between hyperuricemia and diabetes in the United States. *J Clin Med*. 2019;8(12):2127. doi:10.3390/jcm8122127
2. Liang XY, Mei ZG, Wen XD. Analysis of the dispensing pattern of clinical application of SiMiao wan-like formula based on data mining. *Chin Herb Med*. 2022;53(02):507–518. doi:10.7501/j.issn.0253-2670.2022.02.021
3. Yao GZ, Huang Y, Zhang N. Professor Zhang Ning's case study on the application of modified simiao pills. *Chin Med Clin Res*. 2021;13 (31):94–97. doi:10.3969/j.issn.1674-7860.2021.31.026
4. Jia P, Chen G, Yang J, Qin WY. Study on the effect of Simiao Pills on inflammation development and regulation of macrophage polarization in rats with gouty arthritis. *Chin J Trad Chin Med*. 2022;37(06):3498–3502.
5. Lin Y, Zhang N, Zhang J, Lu J, Liu S, Ma G. The association between hydration state and the metabolism of phospholipids and amino acids among young adults: a metabolomic analysis. *Curr Dev Nutr*. 2024;8(3):102087. doi:10.1016/j.cdnut.2024.102087
6. Meng X, Mao Z, Li X, et al. Baicalein decreases uric acid and prevents hyperuricemic nephropathy in mice. *Oncotarget*. 2017;8(25):40305–40317. doi:10.18632/oncotarget.16928
7. Wu H, Zhou M, Lu G, Yang Z, Ji H, Hu Q. Emodinol ameliorates urate nephropathy by regulating renal organic ion transporters and inhibiting immune inflammatory responses in rats. *Biomed Pharmacother*. 2017;96:727–735. doi:10.1016/j.biopha.2017.10.051
8. Hu QH, Zhang X, Wang X, Jiao RQ, Kong LD. Quercetin regulates organic ion transporter and uromodulin expression and improves renal function in hyperuricemic mice. *Eur J Nutr*. 2012;51(5):593–606. doi:10.1007/s00394-011-0243-y
9. Feng X, Sureda A, Jafari S, et al. Berberine in cardiovascular and metabolic diseases: from mechanisms to therapeutics. *Theranostics*. 2019;9 (7):1923–1951. doi:10.7150/thno.30787
10. Shieh DE, Liu LT, Lin CC. Antioxidant and free radical scavenging effects of baicalein, baicalin and wogonin. *Anticancer Res*. 2000;20 (5A):2861–2865.
11. Felser A, Lindinger PW, Schnell D, et al. Hepatocellular toxicity of benzbromarone: effects on mitochondrial function and structure. *Toxicology*. 2014;324:136–146. doi:10.1016/j.tox.2014.08.002
12. Kitagawara Y, Ohe T, Tachibana K, Takahashi K, Nakamura S, Mashino T. Novel bioactivation pathway of benzbromarone mediated by cytochrome P450. *Drug Metab Dispos*. 2015;43(9):1303–1306. doi:10.1124/dmd.115.065037
13. Shirakawa M, Sekine S, Tanaka A, Horie T, Ito K. Metabolic activation of hepatotoxic drug (benzbromarone) induced mitochondrial membrane permeability transition. *Toxicol Appl Pharmacol*. 2015;288(1):12–18. doi:10.1016/j.taap.2015.06.018
14. Waisman J, Mwasi LM, Bluestone R, Klinenberg JR. Acute hyperuricemic nephropathy in rats. An electron microscopic study. *Am J Pathol*. 1975;81(2):367–378.

15. Fang NY, Lv LW, Lv XX, et al. Critical Metabolism Branch of China National Health Association, Multi-disciplinary Expert Group on Diagnosis and Treatment of Hyperuricemia and Related Diseases. China multidisciplinary expert consensus on diagnosis and treatment of hyperuricemia related diseases (2023 Edition). *Chin J Pract Internal Med*. 2023;43(06):461–480. doi:10.19538/j.nk2023060106
16. Doizi S, Poindexter JR, Pearle MS, et al. Impact of potassium citrate vs citric acid on urinary stone risk in calcium phosphate stone formers. *J Urol*. 2018;200(6):1278–1284. doi:10.1016/j.juro.2018.07.039
17. Wang T, Chen T, Cai Q, Chen YZ, Chi XG. Efficacy of febuxostat combined with potassium citrate extended-release tablets in the treatment of gout and hyperuricemia kidney stones. *J Pract Med*. 2020;36(02):224–228. doi:10.3969/j.issn.1006-5725.2020.02.019
18. Peterson JW, Boldogh I, Popov VL, Saini SS, Chopra AK. Anti-inflammatory and antisecretory potential of histidine in Salmonella-challenged mouse small intestine. *Lab Invest*. 1998;78(5):523–534.
19. Smolik S, Nogaj P, Szpakowska A, Lodowska J, Weglarz L. The role of amino acids supplementation of protective Na2H2EDTA containing ointments in chelation of allergenic metal ions. *Acta Pol Pharm*. 2010;67(6):737–740.
20. Ha JW, Choi JY, Boo YC. Differential effects of histidine and histidinamide versus cysteine and cysteinamide on copper ion-induced oxidative stress and cytotoxicity in HaCaT keratinocytes. *Antioxidants*. 2023;12(4):801. doi:10.3390/antiox12040801
21. Zhang ZG, Gao MS, Li JY, et al. Histidine improves ischemia-reperfusion injury in transplanted liver by antioxidant effects. *J Air Force Med Univ*. 2024;45(01):15–21. doi:10.13276/j.issn.2097-1656.2024.01.004
22. Liang M, Wang Z, Li H, et al. L-arginine induces antioxidant response to prevent oxidative stress via stimulation of glutathione synthesis and activation of Nrf2 pathway. *Food Chem Toxicol*. 2018;115:315–328. doi:10.1016/j.fct.2018.03.029
23. Dasgupta T, Hebbel RP, Kaul DK. Protective effect of arginine on oxidative stress in transgenic sickle mouse models. *Free Radic Biol Med*. 2006;41(12):1771–1780. doi:10.1016/j.freeradbiomed.2006.08.025
24. Wang Y, Mei Y, Du R, et al. Arginine as a regulator of antioxidant and gel formation in yak myofibrillar proteins: efficacy and mechanistic insights. *Food Chem X*. 2024;24:101839. doi:10.1016/j.fochx.2024.101839
25. Asakawa S, Shibata S, Morimoto C, et al. Podocyte injury and albuminuria in experimental hyperuricemic model rats. *Oxid Med Cell Longev*. 2017;2017(1):3759153. doi:10.1155/2017/3759153
26. Yip K, Cohen RE, Pillinger MH. Asymptomatic hyperuricemia: is it really asymptomatic? *Curr Opin Rheumatol*. 2020;32(1):71–79. doi:10.1097/BOR.0000000000000679